

Electronic Supplementary Information

Building Artificial Solid Electrolyte Interphase with High-Uniformity and Fast Ion Diffusion for Ultralong-Life Sodium Metal Anodes

Qianwen Chen,^{‡a} Heng He,^{‡ab} Zhen Hou,^a Weiman Zhuang,^a Tianxu Zhang,^a Zongzhao Sun^{ab} and Limin Huang^{*ac}

^a*Department of Chemistry, Southern University of Science and Technology (SUSTech), Shenzhen, Guangdong 518055, China*

^b*School of Chemistry and Chemical Engineering, Harbin Institute of Technology, Harbin 150001, China*

^c*Guangdong Provincial Key Laboratory of Energy Materials for Electric Power, Southern University of Science and Technology, Shenzhen, Guangdong 518055, China*

‡ Both authors have equal contribution.

*E-mail: huanglm@sustech.edu.cn

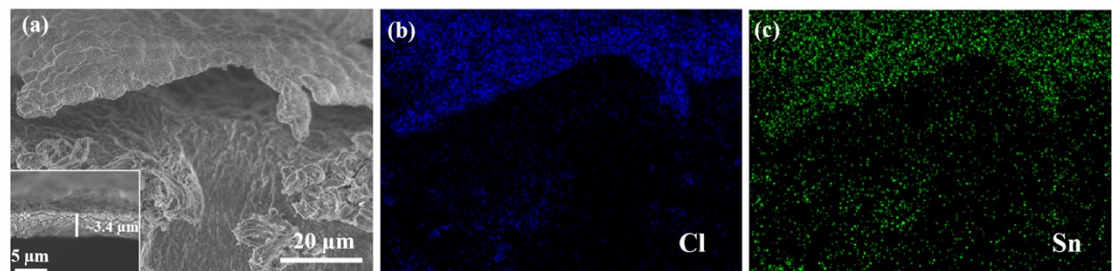


Fig. S1 Cross-sectional SEM image of the $\text{SnCl}_4\text{-Na}$ electrode before cycling and the corresponding EDS elemental mapping of (b) Cl and (c) Sn.

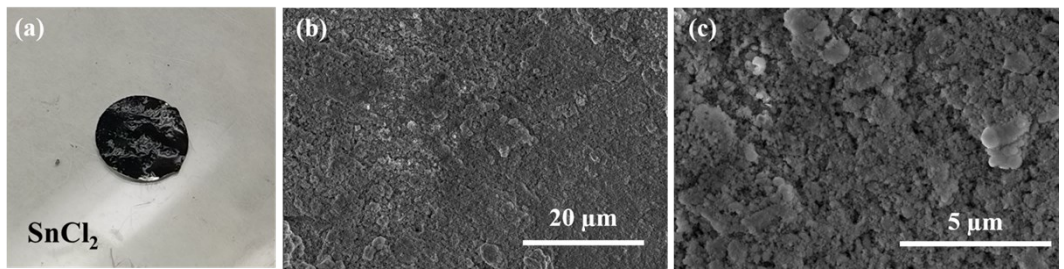


Fig. S2 Optical photo of (a) $\text{SnCl}_2\text{-Na}$ electrode before cycling. (b, c) SEM images of the $\text{SnCl}_2\text{-Na}$ electrode before cycling.

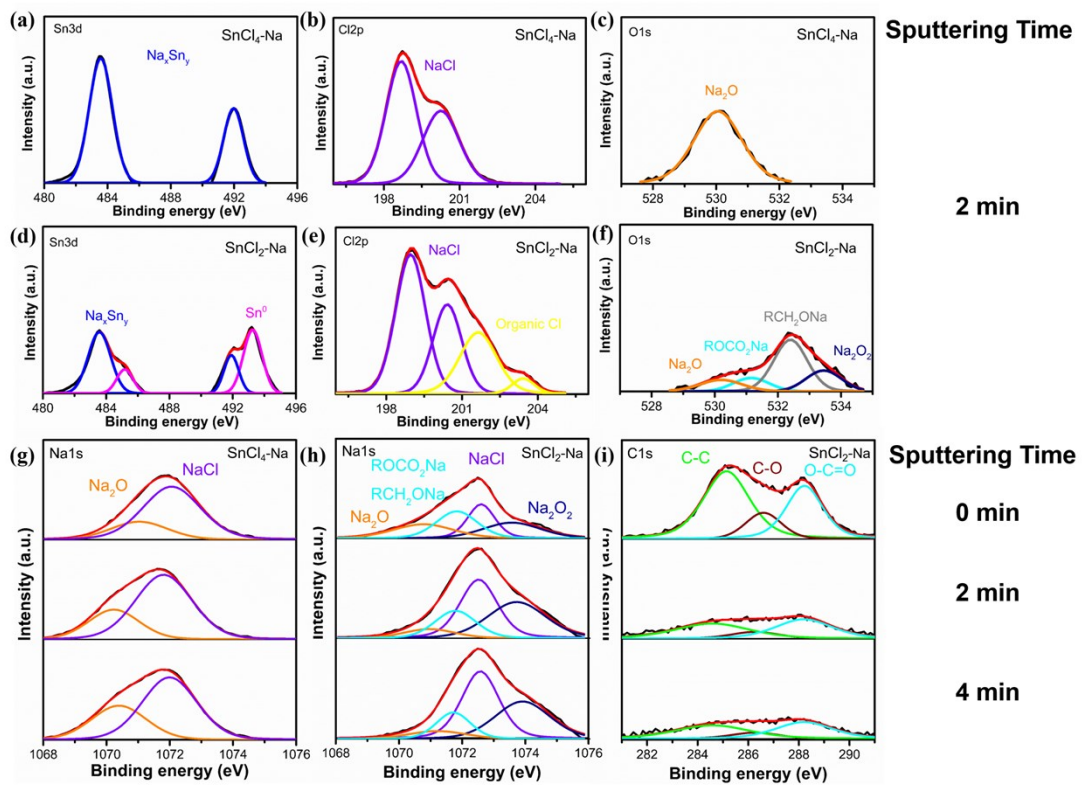


Fig. S3. (a) Sn 3d, (b) Cl 2p and (c) O 1s XPS spectra of the SnCl₄-Na electrode after 2 min Ar cluster ion sputtering. (d) Sn 3d, (e) Cl 2p and (f) O 1s XPS spectra of the SnCl₂-Na electrodes after 2 min Ar sputtering. (g) XPS Na 1s spectra of SnCl₄-Na electrodes before cycling. (h) Na 1s and (i) C 1s XPS spectra of SnCl₂-Na electrode before cycling. (sputtering times are shown in the columns).

The Na 1s spectra of SnCl₄-Na electrode at ~1072.1 eV and ~1070.6 eV are assigned to NaCl and Na₂O.^{1,2} For SnCl₂-Na electrode, the Na 1s spectra are deconvoluted into four peaks at ~1070.9 eV (Na₂O), ~1073.7 eV (Na₂O₂), ~1072.5 eV (NaCl) and ~1071.7 eV (RCH₂ONa and ROCO₂Na),^{3,4} and peaks at ~284.8 eV, ~286.5 eV and ~288.2 eV in C 1s spectra belong to C-C, C-O and O-C=O.²

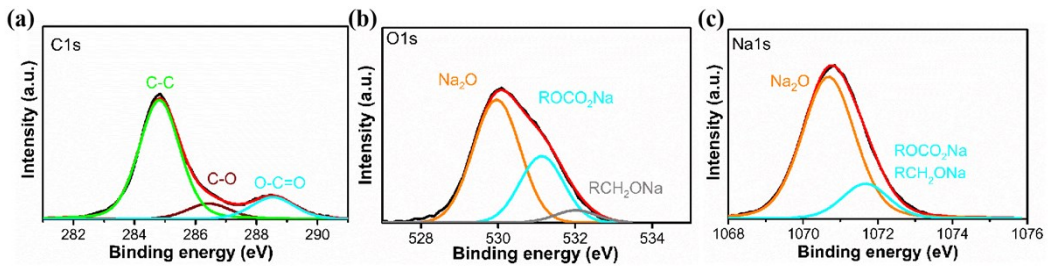


Fig. S4 (a) C 1s, (b) O 1s and (c) Na 1s XPS spectra of the DGM-Na electrode.

The XPS spectra of DGM modified Na metal electrode (DGM-Na electrode) are collected in Fig. S4. In O 1s spectra, the reaction between Na and DGM results in the formation of ROCO₂Na (531.1 eV), RCH₂ONa (532.0 eV) and Na₂O (530.0 eV). These constituents (ROCO₂Na and RCH₂ONa) are similar to the organic species of SEI layer on the SnCl₂-Na electrode, demonstrating that the formed artificial protection layer on SnCl₂-Na electrode surface is attributed to the heterogeneous reaction among Na metal, SnCl₂ and DGM solvent.

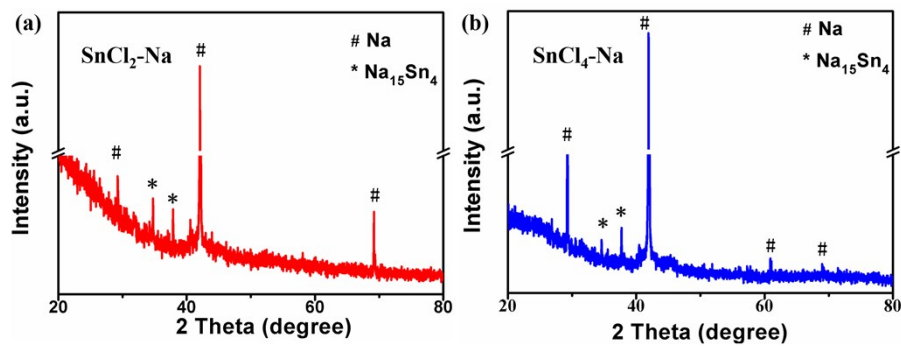


Fig. S5 XRD patterns of (a) $\text{SnCl}_2\text{-Na}$ and (b) $\text{SnCl}_4\text{-Na}$ electrodes.

As shown in Fig. S5, the $\text{SnCl}_2\text{-Na}$ and $\text{SnCl}_4\text{-Na}$ electrodes exhibit characteristic diffraction peaks at 34.8° and 37.5° corresponding to the (511) and (521) facets of the $\text{Na}_{15}\text{Sn}_4$ alloy (PDF #31-1327).

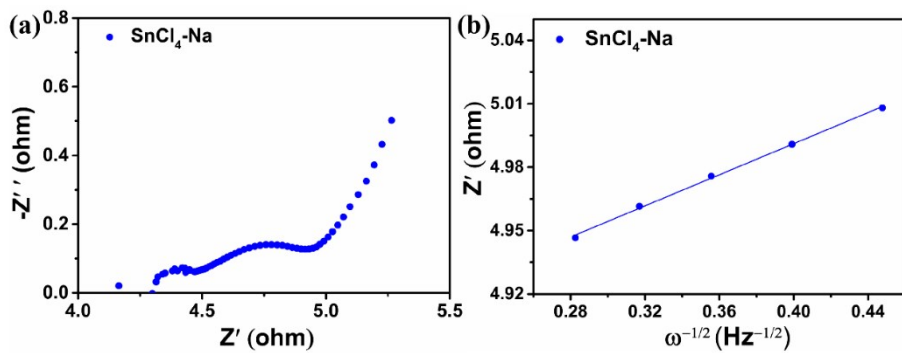


Fig. S6 (a) Nyquist plots of the $\text{SnCl}_4\text{-Na}$ electrode before cycling. (b) Relationship between Z' with $\omega^{-1/2}$ in the low-frequency region for the $\text{SnCl}_4\text{-Na}$ electrode.

The Na^+ ion diffusion coefficients of inorganics (Na-Sn alloy and NaCl) can be obtained from the oblique lines in the low-frequency regions of the Nyquist plots according to the following Eq. 1 and 2:

$$Z' = R_s + R_{ct} + \sigma \omega^{-1/2} \quad (\text{Eq. 1})$$

$$D = R^2 T^2 / (2C^2 F^4 S^2 \sigma^2) \quad (\text{Eq. 2})$$

where the Z' is the real part of impedance, R_s is the Ohm resistance, R_{ct} is the charge transfer resistance, σ is the Warburg factor, ω the angular frequency, D is the Na^+ ion diffusion coefficient, R is the gas constant, T is the absolute temperature, C is the molar concentration of Na^+ ions in the electrolyte, F is the Faraday's constant, and S is the surface area of the electrodes. As shown in Fig. S6b, the Z' has a linear relationship with $\omega^{-1/2}$ and σ is determined by the slope of the lines, and thus D could be obtained ($1.1 \times 10^{-7} \text{ cm}^2 \text{ s}^{-1}$).

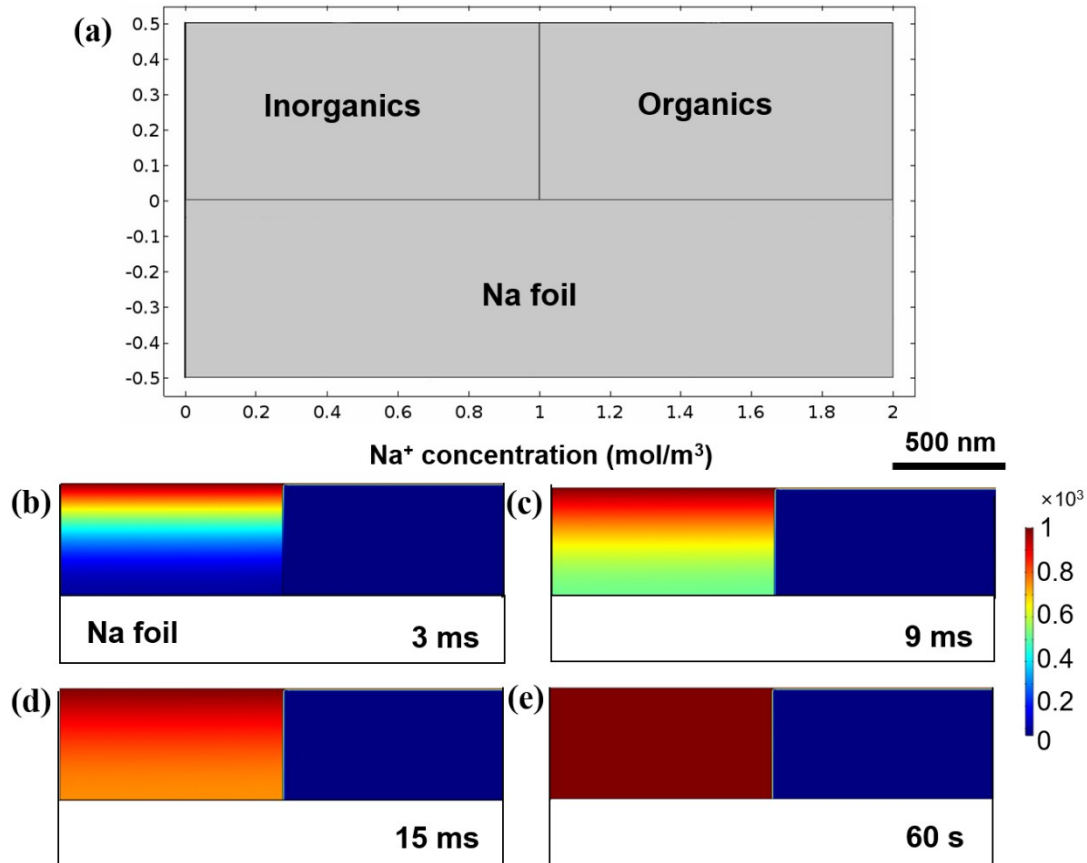


Fig. S7 (a) Simulation of bi-component SEI layer with different diffusion coefficient in COMSOL. (b-e) Simulation of Na^+ concentration in different SEI layer components at different time. Scale bar: 500 nm.

Simulation of different SEI layer components model with thickness 0.5 μm are shown in the in Fig. S7a, and the lengths of inorganics (Na-Sn alloy and NaCl) and organics (ROCO₂Na and RCH₂ONa) are all designed to be 1 μm . The boundary conditions between inorganic and organic blocks are defined continuous boundary condition, in which the concentration at the interface satisfies the following equation:

$$c_{\text{Na}}^+ = c_{\text{Na}}^- \quad (+ \text{ and } - \text{ represent the left and right of the boundary}).$$

The Na^+ concentration in the different protective layer components can be calculated using Fick's law. To simplify the simulation complexity, the convective mass transport and electro-chemical polarization are ignored.

$$\frac{\partial c}{\partial t} = \nabla \cdot (D_i \nabla c) \quad (\text{Eq. 3})$$

where c is Na^+ concentration, and D_i is the Na^+ ion diffusion coefficient in different components.

According to the previous reports⁵, the conductivities of organics (Na alkyl carbonates) is $\sim 2 \times 10^{-12} \text{ S cm}^{-1}$. In addition, the conductivity for all Na alkyl carbonates are identical regardless of chain length at 20 °C. Using following Eq. 4 and 5, a diffusion coefficient of organics ($5.2 \times 10^{-16} \text{ cm}^2 \text{ s}^{-1}$) is obtained.

$$\sigma = \mu n e \quad (\text{Eq. 4})$$

$$D = \frac{\mu k_b T}{q} \quad (\text{Eq. 5})$$

where the σ is the Na^+ ion conductivity, μ is the Na^+ ion mobility, n is the number density of electrons, e is the charge of an electron, D is the Na^+ ion diffusion coefficient, k_b is the Boltzmann constant, T is the absolute temperature, q is the charge of Na^+ ion.

In short, the diffusion coefficients of Na^+ in the organics and inorganics are $5.2 \times 10^{-16} \text{ cm}^2 \text{ s}^{-1}$ and $1.1 \times 10^{-7} \text{ cm}^2 \text{ s}^{-1}$, respectively.

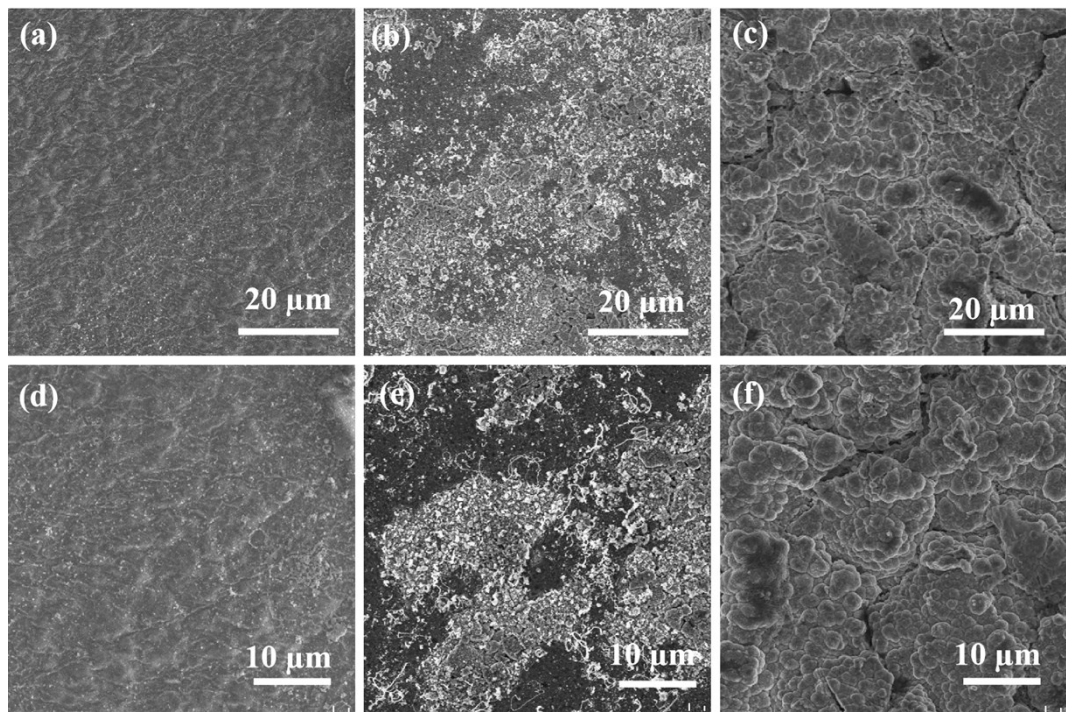


Fig. S8 SEM images of (a, d) the Na, (b, e) SnCl₂-Na and (c, f) SnCl₄-Na electrodes after 100 cycles at 2 mA cm⁻² with a cycling capacity of 1 mAh cm⁻².

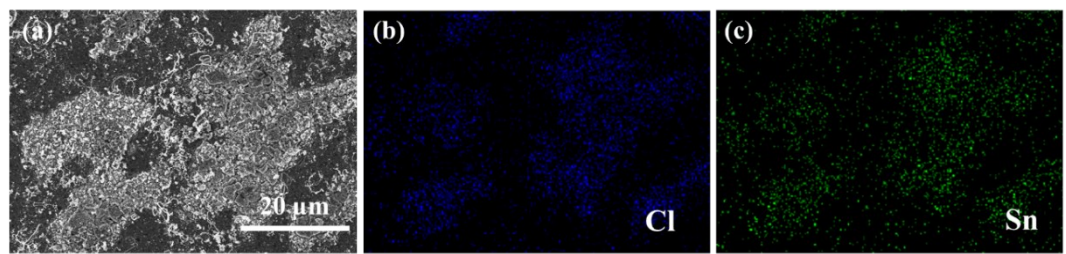


Fig. S9 (a) SEM images of the $\text{SnCl}_2\text{-Na}$ electrode after 100 cycles at 2 mA cm^{-2} with a cycling capacity of 1 mAh cm^{-2} , and the corresponding EDX elemental mappings of (b) Cl and (c) Sn.

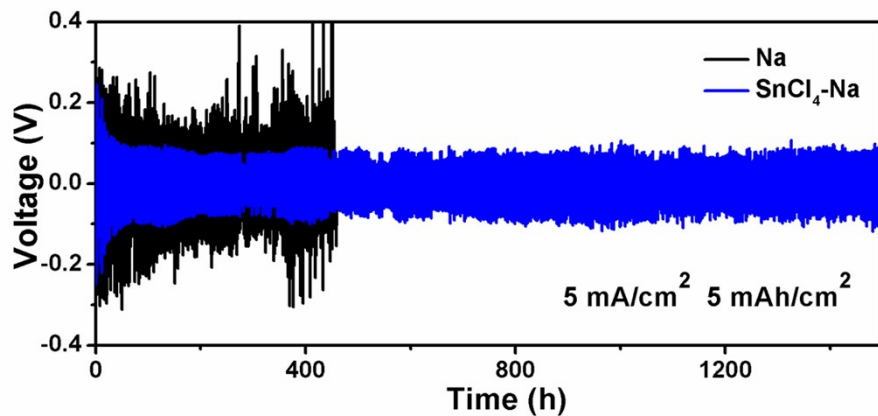


Fig. S10 Cycling performance of the symmetric cells with the Na and SnCl₄-Na electrodes with cycling capacities of 5 mAh cm⁻² at 5 mA cm⁻².

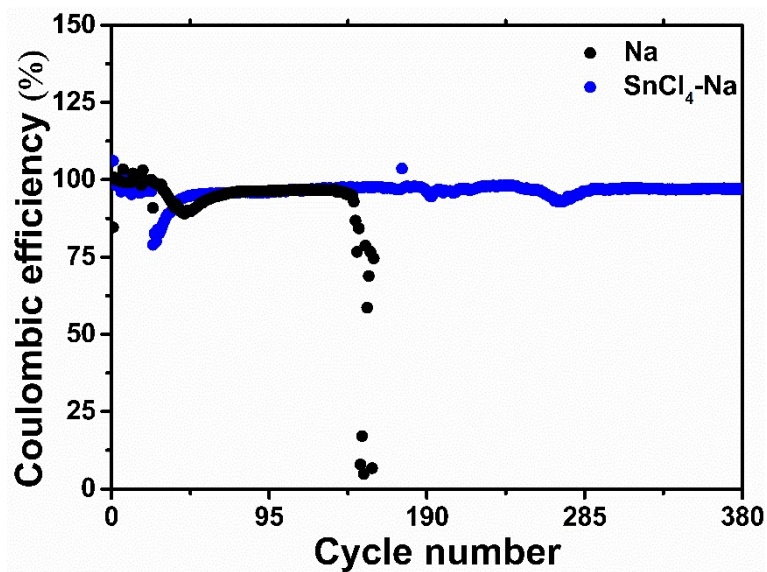


Fig. S11 Coulombic efficiency of Na-FeS₂ full cells using Na and SnCl₄-Na as anodes and FeS₂ as cathodes at 0.2, 0.5, 1, 2 and 0.2 A g⁻¹.

Table S1. Summary of cycle performance of Na plating/stripping behaviors. (The electrolyte concentration is 1M)

Materials	Capacity (mAh/cm ²)	Current density (mA/cm ²)	Cycles	Time (h)	Electrolyte	Refs
Na-Sn alloy/Na ₂ O	1	1	350	700	NaCF ₃ SO ₃ in diglyme	6
		2	500	500		
Na/NSCNT	1	1	250	500	NaSO ₃ CF ₃ in diglyme	7
PhS ₂ Na ₂ -rich protection layer	1	1	400	800	NaPF ₆ in EC/PC	8
		5	700	280		
CNT/Na	1	0.5	200	800	NaClO ₄ in EC/PC	9
MOF/Cu	1	1	300	600	NaClO ₄ in EC/DMC	10
Zn _{SA} -N-C	1	1	150	300	NaClO ₄ in EC/DMC	11
Carbon felt	1	1	550	1100	NaPF ₆ in diglyme	12
		2	350	350		
NaAsF ₆ additive	1	0.5	87	350	NaTFSI in FEC	13
	0.5	0.25	137	550		
Na/CNF	1	1	1000	2000	NaPF ₆ in diglyme	14
SbF ₃ additive	0.5	0.5	500	1000	NaFSI in DME	15
NaI SEI	0.75	0.25	83	500	NaCF ₃ SO ₃ in diglyme	16
NaPS layers	1	1	135	270	NaPF ₆ in EC/PC	17
	3	1	41	250		
Sn-Na alloy	1	0.25	125	1000	NaPF ₆ in EC/PC	18
NaBr interphase	0.25	0.5	250	250	NaPF ₆ in EC/PC	19
Al ₂ O ₃ -PVDF-HFP coating	1	0.5	100	400	NaClO ₄ in EC/PC	20
SnCl ₄ -Na electrode	1		4500	4500	NaPF ₆ in diglyme	This work
	3	2	1333	4000		
	5		600	3000		
	1		7000	2800		
	5	5	750	1500		

Reference

1. Z. W. Seh, J. Sun, Y. Sun and Y. Cui, *ACS Cent. Sci.*, 2015, **1**, 449-455.
2. X. Zheng, H. Fu, C. Hu, H. Xu, Y. Huang, J. Wen, H. Sun, W. Luo and Y. Huang, *J. Phys. Chem. Lett.*, 2019, **10**, 707-714.
3. K. Li, J. Zhang, D. Lin, D. W. Wang, B. Li, W. Lv, S. Sun, Y. B. He, F. Kang, Q. H. Yang, L. Zhou and T. Y. Zhang, *Nat. Commun.*, 2019, **10**, 725.
4. L. L. Marciniuk, P. Hammer, H. O. Pastore, U. Schuchardt and D. Cardoso, *Fuel*, 2014, **118**, 48-54.
5. L. Schafzahl, H. Ehmann, M. Kriechbaum, J. Sattelkow, T. Ganner, H. Plank, M. Wilkening and S. A. Freunberger, *Chem. Mater.*, 2018, **30**, 3338-3345.
6. X. Zheng, W. Yang, Z. Wang, L. Huang, S. Geng, J. Wen, W. Luo and Y. Huang, *Nano Energy*, 2020, **69**, 104387.
7. B. Sun, P. Li, J. Zhang, D. Wang, P. Munroe, C. Wang, P. H. L. Notten and G. Wang, *Adv. Mater.*, 2018, **30**, 1801334.
8. M. Zhu, G. Wang, X. Liu, B. Guo, G. Xu, Z. Huang, M. Wu, H. K. Liu, S. X. Dou and C. Wu, *Angew. Chem. Int. Ed.*, 2020, **59**, 6596-6600.
9. Y.-J. Kim, J. Lee, S. Yuk, H. Noh, H. Chu, H. Kwack, S. Kim, M.-H. Ryou and H.-T. Kim, *J. Power Sources*, 2019, **438**, 227005.
10. J. Qian, Y. Li, M. Zhang, R. Luo, F. Wang, Y. Ye, Y. Xing, W. Li, W. Qu, L. Wang, L. Li, Y. Li, F. Wu and R. Chen, *Nano Energy*, 2019, **60**, 866-874.
11. T. Yang, T. Qian, Y. Sun, J. Zhong, F. Rosei and C. Yan, *Nano Lett.*, 2019, **19**, 7827-7835.
12. J. Zhang, W. Wang, R. Shi, W. Wang, S. Wang, F. Kang and B. Li, *Carbon*, 2019, **155**, 50-55.
13. S. Wang, W. Cai, Z. Sun, F. Huang, Y. Jie, Y. Liu, Y. Chen, B. Peng, R. Cao, G. Zhang and S. Jiao, *Chem. Commun.*, 2019, **55**, 14375-14378.
14. J. Sun, M. Zhang, P. Ju, Y. Hu, X. Chen, W. Wang and C. Chen, *Energy Technology*, 2020, **8**, 1901250.
15. W. Fang, H. Jiang, Y. Zheng, H. Zheng, X. Liang, Y. Sun, C. Chen and H. Xiang, *J. Power Sources*, 2020, **455**, 227956.
16. H. Tian, H. Shao, Y. Chen, X. Fang, P. Xiong, B. Sun, P. H. L. Notten and G. Wang, *Nano Energy*, 2019, **57**, 692-702.
17. Y. Zhao, J. Liang, Q. Sun, Lyudmila V. Goncharova, J. Wang, C. Wang, K. R. Adair, X. Li, F. Zhao, Y. Sun, R. Li and X. Sun, *J. Mater. Chem. A*, 2019, **7**, 4119-4125.
18. S. Choudhury, S. Wei, Y. Ozhabes, D. Gunceler, M. J. Zachman, Z. Tu, J. H. Shin, P. Nath, A. Agrawal, L. F. Kourkoutis, T. A. Arias and L. A. Archer, *Nat. Commun.*, 2017, **8**, 898.
19. Z. Tu, S. Choudhury, M. J. Zachman, S. Wei, K. Zhang, L. F. Kourkoutis and L. A. Archer, *Nat. Energy*, 2018, **3**, 310-316.
20. Y. J. Kim, H. Lee, H. Noh, J. Lee, S. Kim, M. H. Ryou, Y. M. Lee and H. T. Kim, *ACS Appl. Mater. Interfaces*, 2017, **9**, 6000-6006.